Proceedings of Global Power and Propulsion Society
ISSN-Nr: 2504-4400
GPPS Xi'an21
18th–20th October, 2021

www.gpps.global

GPPS-TC-2021-no.175

Effects of Squealer Width and Height on Aerodynamic Performance of Tip-Leakage Flow of Cavity Tips

Xiaojuan He
School of Energy & Power Engineering, Beihang University
hexiaojuan@buaa.edu.cn
Beijing, China

Zhengping Zou
School of Energy & Power Engineering, Beihang University
zouzhengping@buaa.edu.cn
Beijing, China

ABSTRACT

The scraping vortex (SV) is the dominant flow structure in the cavity tip gap. As the basic geometric parameters, it is of great significance to explore the influence mechanism of the squealer width and height on the evolution of SV. In this study, the influence mechanism of the squealer width and height on the SV evolution and aerodynamic performance in a typical transonic high-pressure turbine stage is investigated numerically, which is obtained by analyzing the influences of squealer width and height on the pressure distribution in the tip region, SV characteristics, and tip-leakage performance. The results show that decreasing squealer width or increasing squealer height reduces the transverse pressure gradient (TPG) in the cavity gap, which draws SV to the suction side squealer (SSS) and makes it easier to flow out of the cavity. Moreover, a thinner or a higher squealer leads to a smaller streamwise pressure gradient (SPG) in the cavity, and then the SV intensity enhances and size reduces accordingly. Extensive analysis reveals that there are optimum values of squealer width and height producing the most aerodynamic performance benefits.

INTRODUCTION

In the passage of high-pressure axial turbine, the inevitable over-tip leakage flow not only reduces the work of tip and blocks the main flow(Zou et al., 2018), but also produces mixing loss with the main flow which occupies about one-three of the total loss in blade channel(Denton, 1993). For unshroud blades, the cavity tip has been widely applied to reduce tip-leakage loss(Bunker, 2006).

Compared to flat tip, cavity tip is commonly recognized to perform excellently in controlling tip-leakage loss. When the air flows over two squealers, separation bubbles are generated, resulting in two blockages of tip-leakage flow. Besides, when entering into the cavity, tip-leakage flow mixes with the flow structures in the cavity intensively. Therefore, compared to flat tips, cavity tips produce a smaller discharge coefficient and related tip-leakage loss(Heyes et al., 1992; Chen et al., 1993). Subsequently, deep investigation of flow physics in cavity tip has been performed by quit a few researchers(Zhou, 2015; Virdi et al., 2015). It is discovered that there are many vortices inside the cavity, such as the pressure corner vortex, the suction corner vortex, the scraping vortex. Zou et al.(Zou et al., 2017) showed that SV is the dominant flow structure in controlling leakage flow, which blocks over-tip leakage flow like an aero-labyrinth resulting the decrease of discharge coefficient and tip-leakage loss accordingly. Furthermore, a kinematic model of SV was also established by authors(Zou et al., 2020). Subsequently, the existence of SV and its dominance in controlling tip-leakage flow is verified experimentally in a cascade with a cavity tip(Zeng et al., 2020). However, the generation and evolution mechanism of SV is not fully understood yet.

The change of cavity geometry has an important impact on the flow physics in the gap and tip-leakage loss(Coull et al., 2014; Du et al., 2019). As the basic geometric parameters, it is of great significance to determine the squealer width and height effectively. For the cavity tip with a uniform squealer width and height, the squealer width has a weaker effect on turbine aerodynamic performance, while the influence of squealer height is more significant and complex(Zhou and Hodson, 2012; Senel et al., 2018). Zou et al.(Zou et al., 2017) revealed that the characteristics of SV changes with the variation of squealer height, which alter the ontrolling effect of tip-leakage loss. Besides, quit a few studies investigated the optimization of cavity geometry to improve aerodynamic erformance of turbine further(Pátý et al., 2018; Maral et al., 2019). For instance, Prakash et al.(Schabowski et al., 2014) proposed a ew cavity geometry where the pressure side squealer

(PSS) is inclined, which causes a larger flow separation at the top of pressure side quealer compared to a baseline cavity tip. In consequence, the new cavity geometry strengthens the blockage of over-tip leakage flow. From hese studies, it is obvious that organizing the flow in the tip region reasonably by optimizations of cavity geometry has produced certain aerodynamic benefits successfully. Nonetheless, the emphases of current published studies are primarily laid on the impacts of cavity geometry on the flow patterns in the tip region and tip-leakage aerodynamic performance, while the investigation of generation and evolution echanism of important flow structures in the cavity gap is rare yet.

From point of view of the dominant flow structure, the influence mechanism of squealer width and height on SV evolution and turbine aerodynamic performance are investigated numerically in this paper. The two geometric parameters are related to the pressure distribution and SV evolution in the cavity, and then the influence of SV evolution on leakage flow control is further explained.

METHODOLOGY

Turbine models

TTM single stage turbine (Erhard, 2000) , a typical transonic turbine, is used in this study, of which sketch is shown in Fig.1(a)(Go¨ttlich et al., 2004). The main geometric features and the boundary conditions are described in Table1. Fig.1(b) and (c) show the sketch of cavity tip and the definition of geometric parameters respectively. Then, the study of effects of squealer width and height on the tip-leakage flow is performed based on the cavity tip with a pressure side squealer (PSS) rim of 30°inclination angle. The squealer width and height of different cavity tips are listed in Table2.

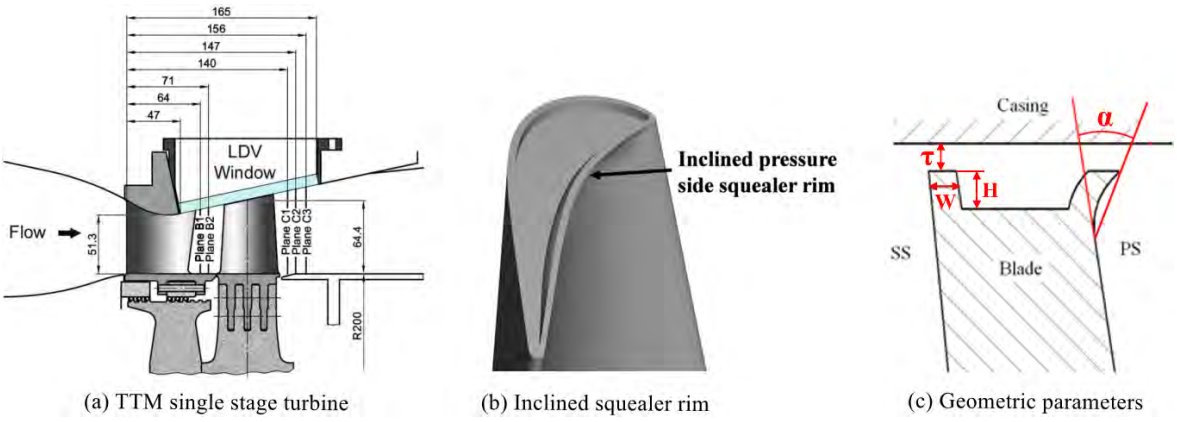

(a) TTM single stage turbine (b) Inclined squealer rim (c) Geometric parameters

Figure 1 Sketches of TTM single stage turbine and cavity tip.

Table 1 Main geometric characteristics and boundary conditions of TTM stage.

	Blade number	Aspect ratio	τ/h	Zweifel's coefficient
stator	24	0.78	-	0.67
rotor	36	1.35	1.40%	0.94
π	$T0_{inlet}/K$	$n/(rpm)$	$\dot{m}_{leakage}/(kg/s)$	Re
3.12	454.4	11000	18.1	1.6×10e6

Definition of important parameters

In this study, the tangential direction of the camber line at the blade top is defined as the streamwise direction, while the direction perpendicular to the camber line as the transverse direction. All the streamwise sections are perpendicular to the camber line.

The leakage flow rate and momentum differences per unit length can be defined as follows, where the isotropic velocity at 95% span suction side blade surface is used to assume the main flow velocity:

$$\dot{m}_{leakage} = \frac{\int \rho V_N dA_e}{\int dl} \tag{1}$$

$$\Delta\left(\dot{m}_{leakage} V\right) = \frac{\int \rho V_N V_{diff} dA_e}{\int dl} \tag{2}$$

Table 2 Squealer width and height of different cavity tips.

Turbine	Squealer width and height
W0.5H1.5	W=1.0τ, H=1.5τ
W1.0H1.5	W=0.5τ, H=1.5τ
W1.5H1.5	W=1.5τ, H=1.5τ
W1.0H0.5	W=1.0τ, H=0.5τ
W1.0H2.5	W=1.0τ, H=2.5τ

The tip-leakage loss is calculated as follows:

$$Y_{tip} = \dot{m}_{passagenotip} T_{2notip} \Delta S_{notip} - \dot{m}_{passage} T_2 \Delta S \tag{3}$$

The total-pressure loss coefficient is described as:

$$C_{pt} = \frac{P_1^* - P^*}{0.5 \rho_2 V_2^2} \tag{4}$$

Computational setup and grid

Numerical methods are widely used in the study of aerodynamic performance of high-pressure turbine, which is capable to predict the tip-leakage aerodynamic performance and describe the flow physics of tip-leakage flow well(Lei et al., 2010; Zou et al., 2017). In the current study, the numerical simulation is performed by using commercial software ANSYS CFX to solve steady Reynolds-averaged Navier-Stokes (RANS) equations. The SST k-ω turbulence model is used to close these equations. The computational domain is shown in Fig.2, containing a stator channel and a rotor channel. The inlet boundary conditions are set as total temperature(454.5K), otal pressure($3.44 \times 10^5 Pa$), inflow angle(0°) and turbulence intensity(5%), and the outlet boundary conditions as static ressure. Periodic boundary conditions are applied on both circumferential sides of stator and rotor domains. No slip and adiabatic oundary conditions are used on all walls.

The software Numeca Autogrid5 is employed to generate domain meshes. An H-O-H grid topology is used for all different cavity tip turbines, illustrated in Fig.2. The thickness of first mesh cell is set as 0.001 mm making the average of y+ about 1.2. To avoid the numerical discrepancy caused by different mesh density, the grid independency study is performed by five different mesh numbers, listed in Table3. According to Table3, the leakage flow rate variation is less than 0.3%, when the mesh number is more than Grid4. Considering the prediction accuracy and calculation cost, Grid4 is employed in this work.

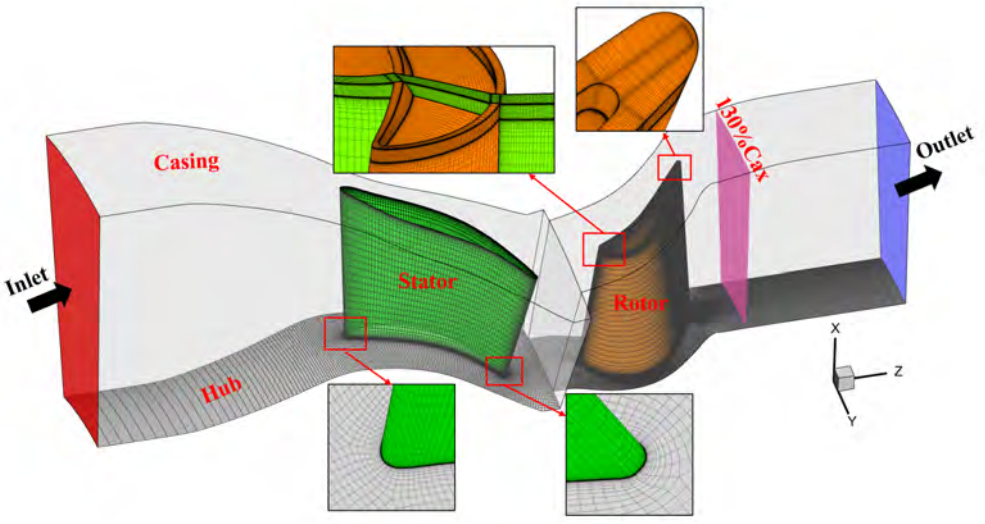

Figure 2 Computational domain and mesh.

Numerical methods validation

The experimental data publicized from Ref.(Mischo et al., 2010) is used for the validation of numerical methods in current study. The validation is performed by comparing the mass flow rate in the passage and turbine power between the

Table 3 Grid independent test.

	Axial×Tangential×Radial		Total Number/×10^6	$\frac{\dot{m}_{leakage}}{\dot{m}_{mainstream}}$/×%
	Stator	Rotor (tip)		
Grid1		121×41×110 (13)	0.89	3.01
Grid2		139×49×125 (21)	1.16	3.07
Grid3	99×55×57	167×57×131 (29)	1.56	3.08
Grid4		185×65×145 (37)	2.05	3.09
Grid5		203×73×161 (45)	2.80	3.09

experimental results(Mischo et al., 2010) and numerical results. Fig.3 shows excellent agreement between the predicted mass flow rates and turbine powers with experiment at different peration conditions. It is demonstrated that the aerodynamic performance of the turbine is predicted accurately enough used by the umerical methods in current study.

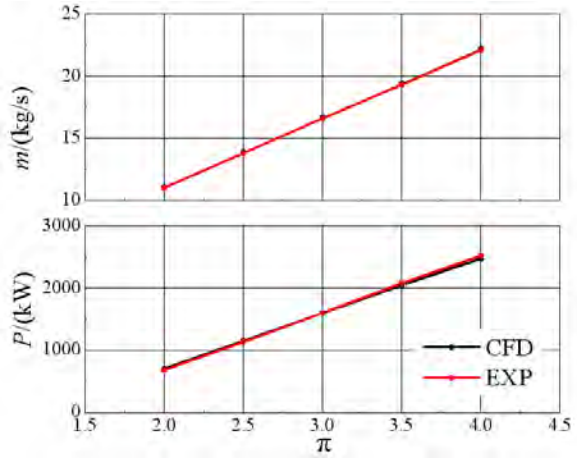

Figure 3 Comparations of (a) mass flow rate and (b)turbine power between numerical and experimental results.

RESULTS AND DISCUSSION

Effects of squealer width on the cavity tip

Pressure distribution

Varied cavity geometry alters the pressure distribution and the SV evolution accordingly in the cavity, and then the tip-leakage performance is affected. In this paper, to explore the influence of squealer width and height on the pressure distribution, both the variation of TPG and SPG are discussed.

Fig.4 gives the contours of TPG at different streamwise sections for with different squealer width. As shown in Fig.4(a), there are two local high adverse TPG zones in the cavity, marked as zone 1 and zone 2 respectively. It is revealed that as the squealer width increases, the influence of the SSS on the zone 1 enhances, then the TPG of zone 1 grows and the distance between zone 1 and zone 2 is cut down gradually; while that of zone 2 barely changes. Besides, it is exposed that the variation of squealer width has a great impact on the TPG on the top of PSS, meaning that the flow condition of cavity inlet is changed. The reason is that when the squealer width is small, under the blocking of the separation vortex on the top of PSS, the equivalent passage of leakage flow is convergent purely. However, when the squealer width is large enough, it acts as a convergent-divergent nozzle, and therefore there is a local adverse TPG zone near the entrance of cavity. The larger the squealer width is, the greater the adverse TPG is. Fig.5 compares the distributions of TPG along the transverse direction in the middle of gaps with different squealer width conditions, in which 0 and 1 on the abscissa axis represent the pressure and suction side of blade surface respectively. As shown in ig.5, as the squealer width increases, the TPG near the entrance of the cavity increases apparently, while that in the avity gap changes barely.

Fig.6 displays the contours of SPG at different streamwise sections in the tip regions with different squealer width. It is shown that, in the upstream of about 30% streamwise position, the cavity is divergent. Hence, the flow in this region is controlled mainly by adverse SPG. With the increase of squealer width, the divergence of the cavity is reduced, and in consequence, the adverse SPG is weakened slightly. In the downstream of the 30% streamwise position, the cavity is convergent, and then the flow is mainly controlled by favorable SPG, and locally by adverse SPG in the meantime. In this region, as the squealer width increases, the enhancement of the action of SSS results in a rise of local adverse SPG. However,

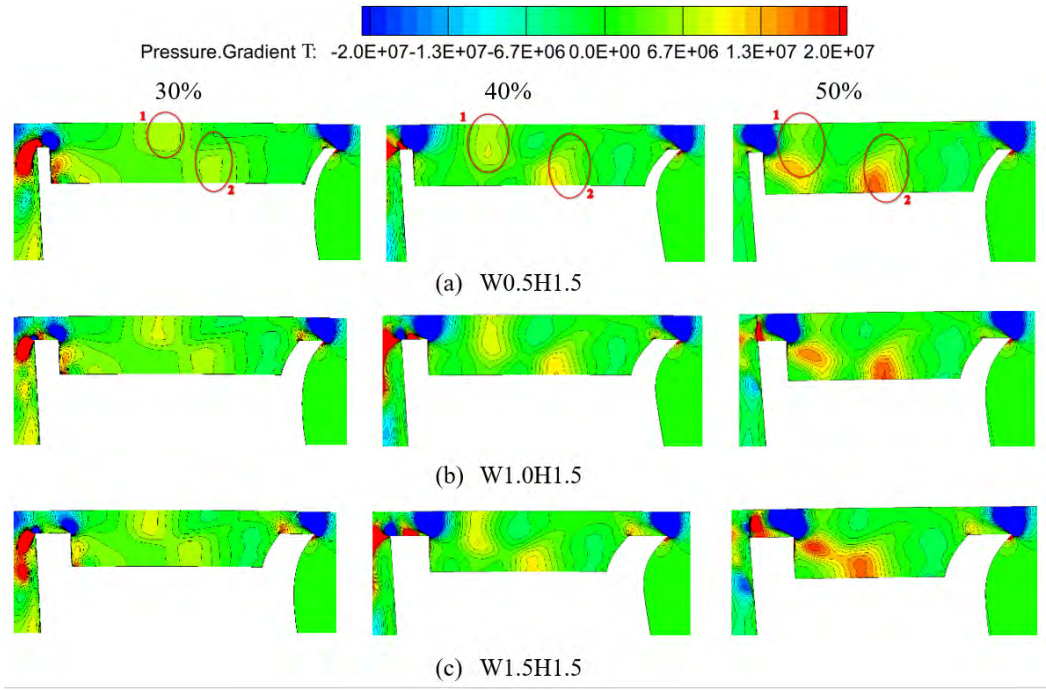

Figure 4 Distributions of TPG at streamwise sections with different squealer width conditions.

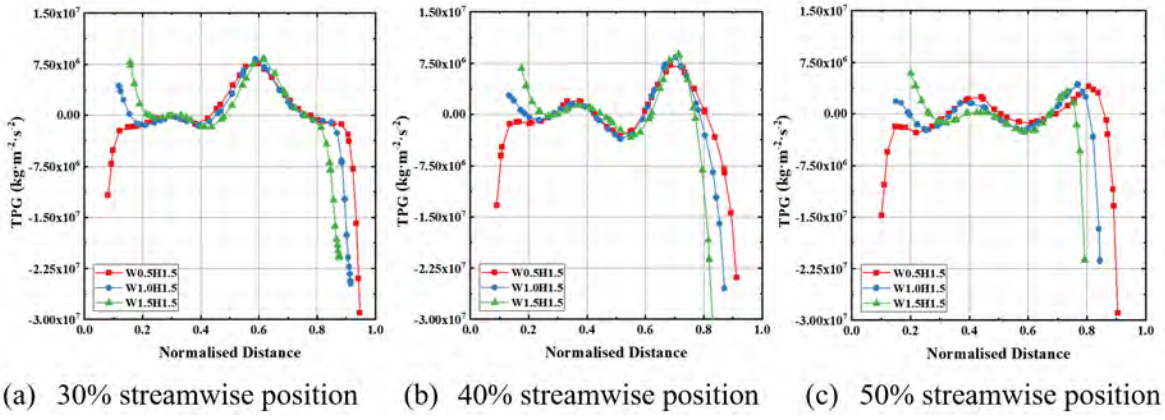

Figure 5 Distributions of TPG along the transverse direction in the middle of gaps for different squealer width.

due to the increase of the contraction of cavity, the favorable SPG in the cavity is enhanced as the increase of squealer width. Besides, it is displayed that the flow near the trailing edge of the cavity is mainly controlled by adverse SPG. The streamwise distributions of the transversely averaged SPG and streamwise velocity in the cavity gap with different squealer width are compared in Fig.7. As shown in Fig.7, along the cavity, the flow in different cavities all has a tendency of first decelerating and pressurized, and then accelerating and depressurized, and finally decelerating and pressurized again. As the squealer idth increases, except for the region near the trailing edge of cavity, because of both the decrease of the diffusion of cavity upstream nd the increase of the convergence of cavity downstream, the SPG is reduced continuously and the streamwise velocity increases accordingly s a whole.

Evolution of SV

Fig.8 describes the distributions of vortex core trajectories, averaged streamwise vorticity and vortex areas of SV with different squealer width conditions. As displayed in Fig.8, although the characteristics of SV change significantly in ifferent cavity tips, the evolution law of SV is similar. Along the cavity, the SV intensity is first enhanced and then weakened, and the ize first increases and then decreases accordingly. Moreover, the SV moves toward the SSS gradually until flowing out of the cavity ompletely.

As is shown in Fig.8(a), as the squealer width increases, along with the increase of the TPG in the gap, the speed of the SV moving to the SSS reduces gradually. It is illustrated that the absolute position is similar for different squealer width.

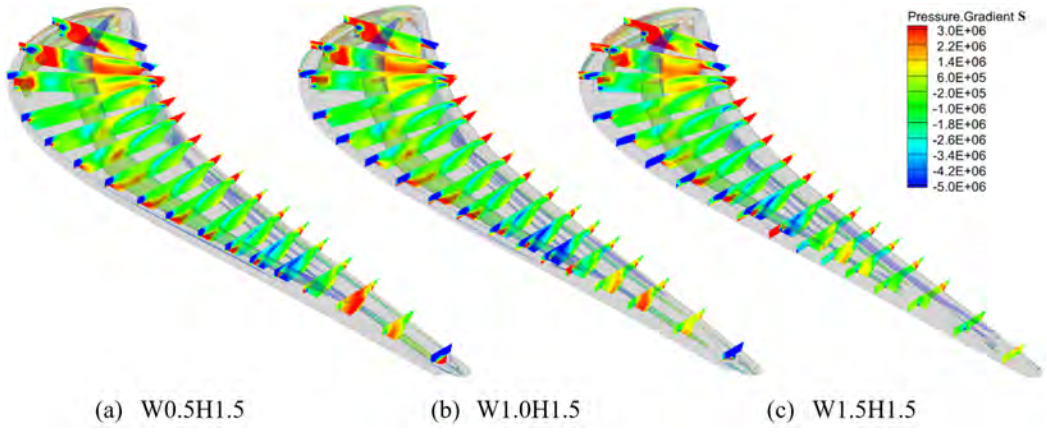

Figure 6 Distributions of SPG at streamwise sections with different squealer width conditions.

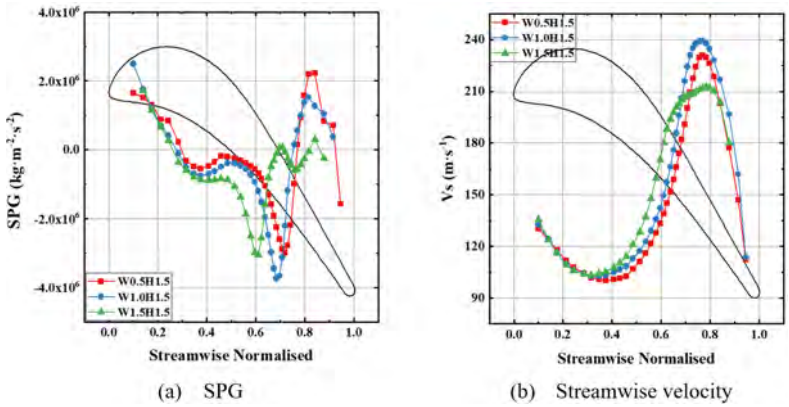

Figure 7 Comparisons of the streamwise distributions of transversely averaged SPG and streamwise velocity in the cavity gaps with different squealer width.

However, at the same streamwise position, the vortex core is closer to the PSS with a smaller squealer width condition. Nevertheless, the increase of squealer width leads to the reduction of the width of the cavity, and in onsequence the SV locates closer to the SSS in the meantime. Under the influences as aforementioned, the vortex cores in different cavity ips almost all arrive at the SSS at 45% streamwise position. However, the reduction of the squealer width draws the SV flow out from avity earlier.

As exhibited in Fig.8 (b) and (c), in the upstream of the 30% streamwise position mainly controlled by adverse SPG, the SV is compressed. Thereby, along the cavity, its intensity reduces and size increases correspondingly. With increasing the squealer width, the adverse SPG decreases, and then the compression of SV is weakened slightly. In the meantime, the enhancement of adverse TPG make a decreasing trend of vorticity and size. Exposed to these two actions, it is shown that the SV intensity is roughly the same in different cavity tips, and the size is reduced slightly. In the 30-45% streamwise region, as continuing to move toward the SSS, the SV is mainly controlled by the local adverse SPG, and then is still compressed. Consequently, the SV intensity decreases and its size increases continuously. When the squealer width increases, under the action of the increase of the local adverse SPG, the favorable SPG and the local adverse TPG in the cavity, the discrepancy of the SV intensity in different cavity tips is tiny, and however its size is gradually restricted by the varied squealer width. In the downstream of the 45% streamwise position mainly controlled by favorable SPG, the SV is stretched. herefore, along the cavity, its intensity increases and size decreases accordingly. With the increase of the squealer width, the favorable PG increases, and then the SV is stretched more apparently. Therefore, the tendency of the SV intensity increasing and size decreasing long the cavity becomes more obvious. It can be seen that, at the same streamwise position, the SV intensity is greater, and size smaller ith a wider squealer rim.

Distributions of leakage flow at the gap outlet

The mixing loss between leakage flow and main flow is related to the leakage flow rate and momentum differences closely(Young and Wilcock, 2002). Therefore, Fig.9 compares distributions of leakage flow rate and momentum differences at the gap outlet with different squealer width conditions. According to Fig.9(a), as the squealer width increases, the influencing scope of SV is reduced gradually. In consequence, the leakage flow rate increases continuously at downstream

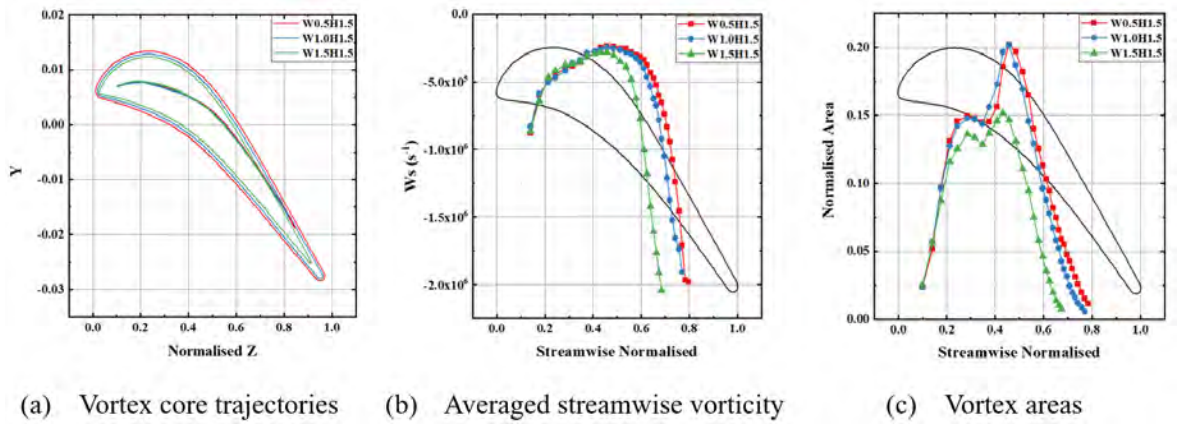

Figure 8 Streamwise distributions of the position, intensity and size of SV for different squealer width.

at the gap outlet. Although the intensity and size of the SV in different cavity tips are quite diverse in the region of no SV exiting, they are almost the same for distributions of leakage flow rate. Based on this phenomenon, it can be revealed that the influencing scope of SV is critical, that is, the larger influencing scope of SV is, the better controlling effect on tip-leakage flow is. The distribution of the leakage flow rate determines that of the normal momentum difference. As shown in Fig.9(b), the ariation of the distribution of normal momentum with the change of squealer width is nearly consistent with that of the leakage flow rate, howing that, with the increase of the squealer width, the normal momentum difference increases gradually downstream at the gap outlet. owever, because the intensity of SV increases slightly, the energy dissipation in the cavity increases gradually. Besides, the decrease of he SPG in the cavity results in the increase of the streamwise velocity at the gap outlet. Therefore, in the influencing scope of the SV, he tangential momentum difference between leakage flow and mainstream is reduced, as shown in Fig.9(c). In other words, as the squealer width increases, the SV influencing scope decreases gradually, but its influencing intensity increases slightly.

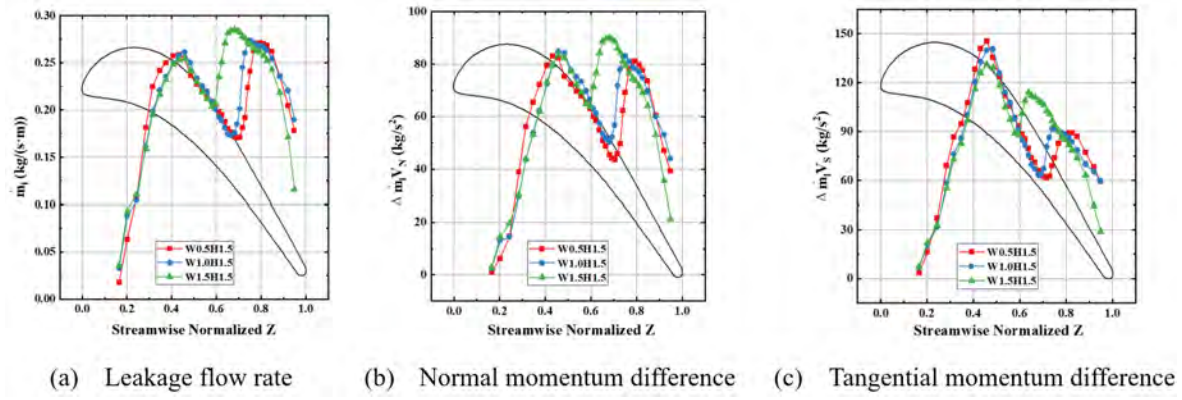

Figure 9 Streamwise distributions of leakage flow rate and momentum differences between leakage flow and mainstream at the gap outlet with different squealer width conditions.

Effects of squealer height on the cavity tip

Pressure distribution

Fig.10 gives the contours of TPG at different streamwise sections in the cavity tips with different squealer height. It is revealed that, as the squealer height increases, the action of the SSS on the zone 1 increases, and in consequence the TPG in the zone 1 grows gradually. In this process, because of the weakening of the influence of the cavity floor, the adverse TPG in the zone 2 has a tendency of reducing. However, in the downstream of the cavity, the enhancement of the influence of the SSS results in the increase of the TPG in the zone 2. In order to promote the influence of the squealer height variation on the TPG in the gap more clearly, the distributions of TPG along the transverse direction in the middle of gap of different cavity tips are displayed in Fig.11. It can be seen that, as the squealer height increases, the TPG in the gap decreases gradually as a whole.

Comparison of the distributions of the SPG at different streamwise sections in cavity gaps with different squealer height is displayed in Fig.12. It is shown that, in the upstream of about 30% streamwise position, as the squealer height increases, the enhancement of the divergence of cavity together with the action of the squealer rim makes the adverse

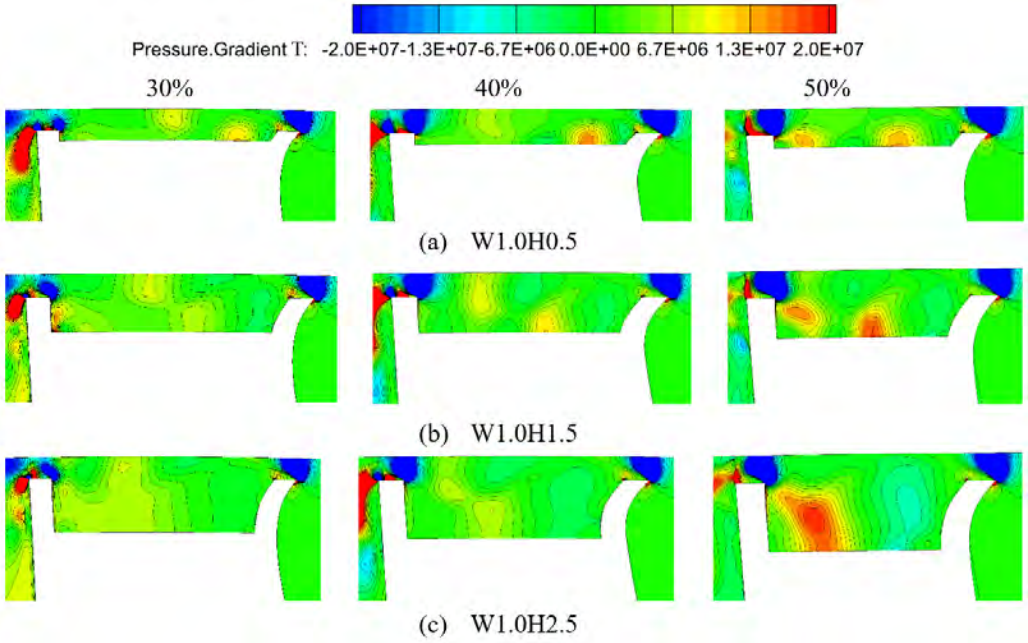

Figure 10 Distributions of TPG at streamwise sections with different squealer height conditions.

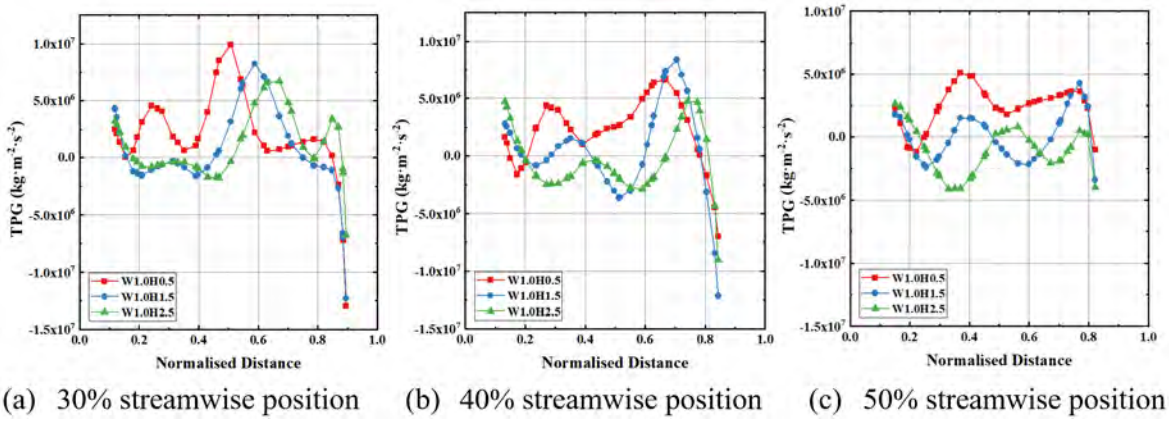

Figure 11 Distributions of TPG along the transverse direction in the middle of gaps for different squealer height.

SPG grow significantly. In the downstream of the 30% streamwise position, with the increase of the squealer height, the convergence of cavity increases in a certain, and therefore the SPG in the cavity has a tendency of increasing. However, the enhancement of the influence of the SSS results in the increase of the local adverse SPG. Ultimately, as shown in Fig.13, as the squealer height increases, the averaged SPG in the cavity continues to increase, and the streamwise velocity decreases correspondingly as a whole.

Evolution of SV

Fig.14 describes the streamwise distributions of the characteristics of SV in the cavities with three different squealer eight. It can be seen that the varied squealer height still does not alter the evolution law of SV, but changes its characteristics bviously. According to Fig.14(a), with the increase of squealer height, along with the decrease of the TPG in the gap, the position f the generation of SV migrates to the SSS gradually, and the speed of SV moving to the SSS along the cavity increases. Therefore, at the ame streamwise position, the SV core is closer to the SSS, and arrives at SSS earlier accordingly which results in the advancement of the position of the SV flowing out of the cavity.

According to Fig.14 (b) and (c), before arriving at the SSS, as the squealer height increases, along with the increase of the adverse SPG in the cavity, the SV is compressed more greatly. Consequently, the SV intensity is smaller, and size larger correspondingly. After SV arriving at the SSS, with the increase of the squealer height, although the favorable SPG in the cavity increase gradually, the enhancement of the local adverse SPG induces the weakening of the SV stretch. Ultimately, the speed of both the SV intensity increasing and the size decreasing drops in a certain. In the meantime, the enhancement of local adverse TPG make the amplitude of intensity increasing smaller, and that of size decreasing bigger. Besides, it is

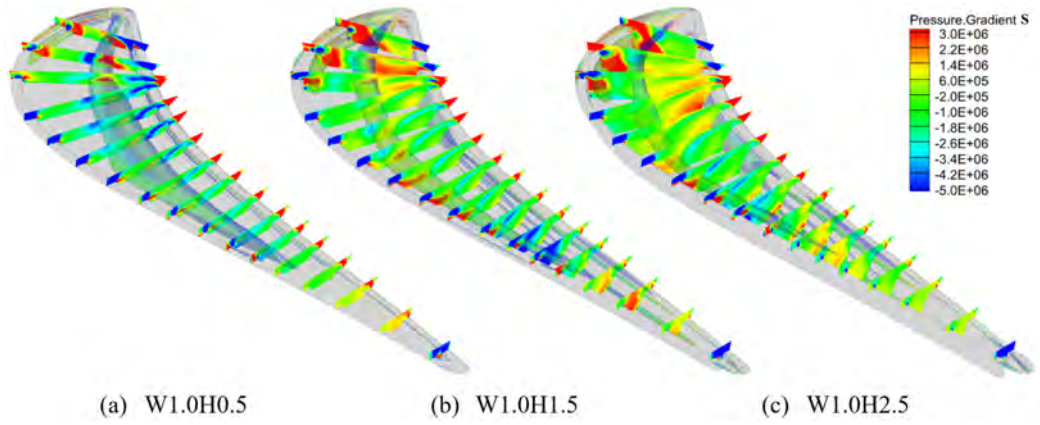

Figure 12 Distributions of SPG at streamwise sections with different squealer height conditions.

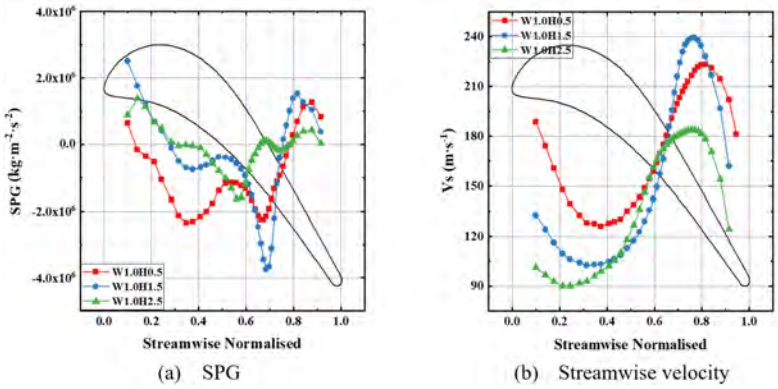

Figure 13 Comparisons of the streamwise distributions of transversely averaged SPG and streamwise velocity in the cavity gaps with different squealer height.

demonstrated that, as the squealer height decreases, the size of SV is restricted gradually by the cavity floor.

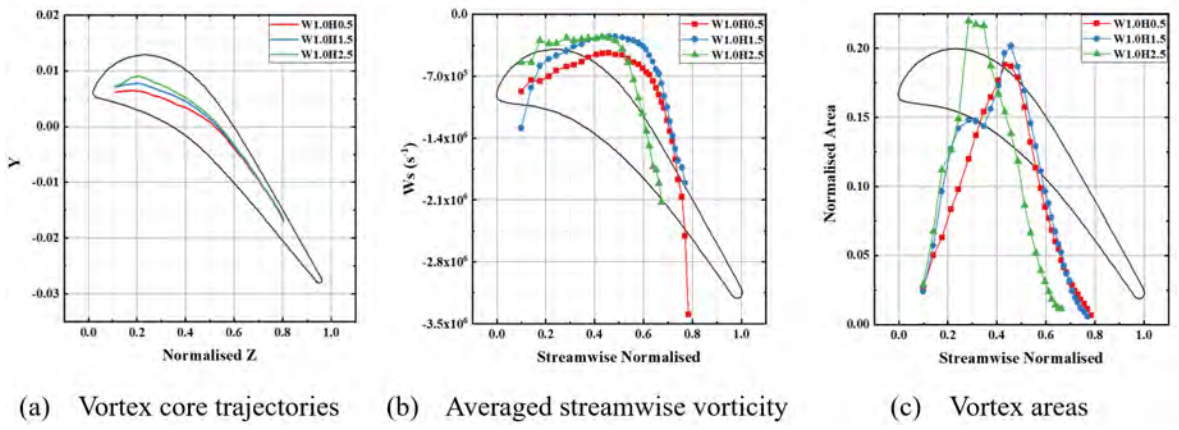

Figure 14 Streamwise distributions of the position, intensity and size of SV with different squealer height conditions.

Distributions of the leakage flow at the gap outlet

Fig.15 shows a comparison of distributions of leakage flow rate and momentum differences between leakage flow and mainstream at the gap outlet for three different squealer height. According to Fig.15 (a), with the increase of squealer height, although the vortex core of the SV is closer to the SSS, the reduction of its size induces the SV in different cavities almost all to arrive at the SSS at 45% streamwise position. Moreover, the advancement of the position of SV flowing out of the cavity results in the increase of the leakage flow rate downstream of the gap outlet. It can be explored that, in the influencing scope of the SV, a SV with a position closer to the SSS produces a more effective blocking effect on the leakage flow, and

in the meantime a larger size induces a greater energy dissipation in the cavity. Under the actions of the two aspects above, the leakage flow rate continues to decrease with the increase of the squealer height in the SV influencing scope.

According to Fig.15 (b) and (c), the variations of the distributions of normal and tangential momentum difference along the streamwise direction with the change of the squealer height are similar with that of the leakage flow rate, showing that, as the squealer height increases, the momentum differences decreases gradually in the influencing scope of the SV, and nevertheless increases downstream of the gap outlet. However, the increase of the SPG in the cavity results in the decrease of the streamwise velocity at the gap outlet, and in consequence the decrease amplitude of the tangential momentum difference is reduced. It can be seen that, there also is an optimum value of the squealer height producing the best controlling effect on the leakage loss.

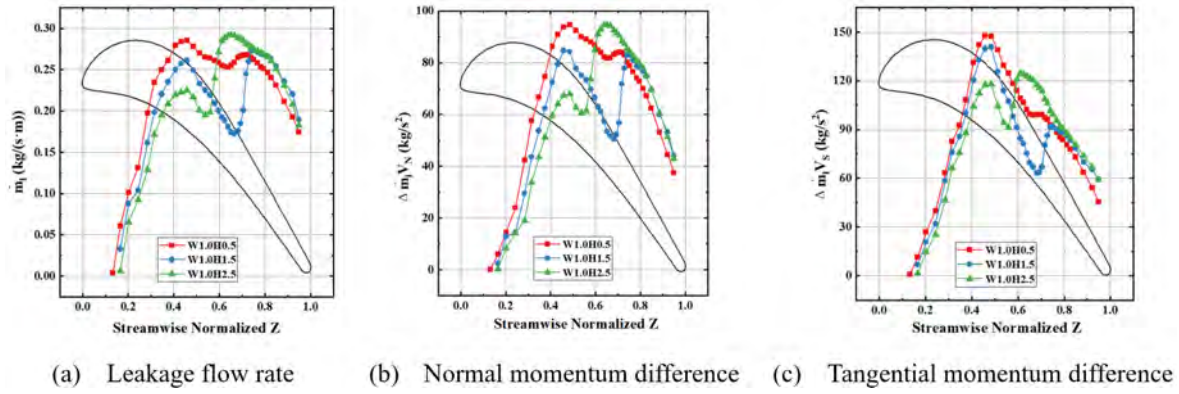

Figure 15 Streamwise distributions of leakage flow rate and momentum differences between leakage flow and mainstream at the gap outlet with different squealer height conditions.

Aerodynamic investigation

In this section, the influence of squealer width and height on turbine aerodynamic performance is investigated. Fig.16 displays the distributions of Cpt at the plane 30%Cax downstream of the rotor. According to Fig.16, high Cpt appears in the leakage vortex (LV) and upper passage vortex (UPV), especially leakage vortex, indicating that the main loss in the upper blade passage deriving from leakage vortex and upper passage vortex. As shown in Fig.16(a), for the cases with different squealer width, the distributions of Cpt are similar, except for a slight variation when the squealer is wider. Compared to squealer width, the influence of squealer height is more significant. As shown in Fig.16(b), with the increase of squealer height, the magnitude of Cpt and size of high Cpt in LV all first decrease remarkably, and then increase gradually. The variation of Cpt in UPV is just opposite to that in LV.

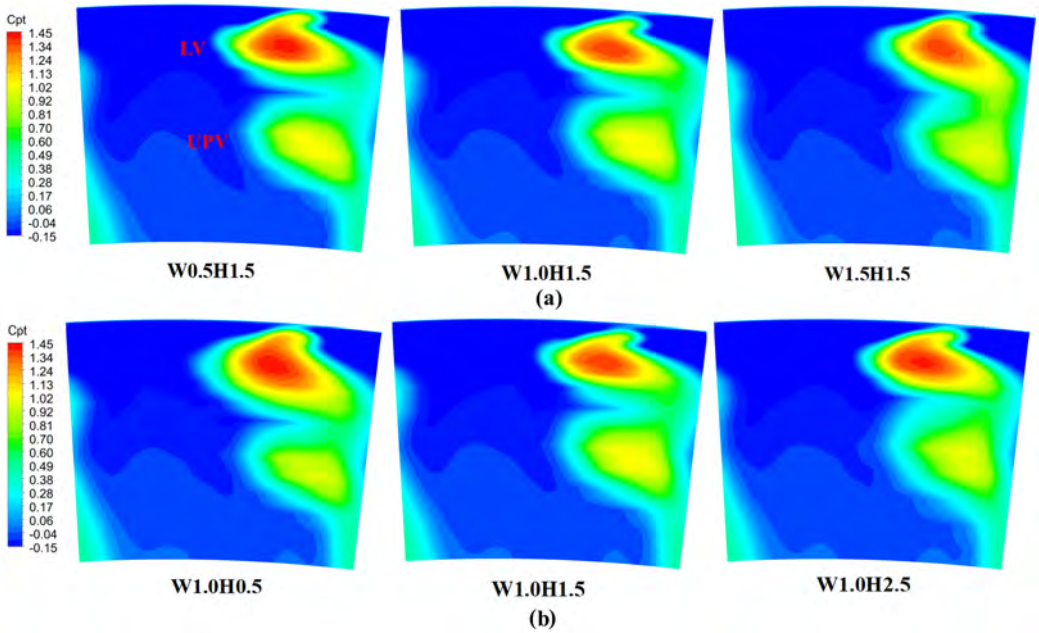

Figure 16 Distributions of total-pressure loss coefficient at the plane 30%Cax downstream of the rotor.

Fig.17 illustrates the distributions of total-pressure loss coefficient at the plane 30%Cax downstream of the rotor. As shown in Fig.17(a), the spanwise range of high Cpt in LV and UPV are so similar in cases with different squealer width. However, with the increase of squealer width, the peak of Cpt in LV reduces slightly due to the reduction of tip-leakage flow, while the high Cpt caused by the interaction of LV and UPV increases monotonously. According to Fig.17(b), it is demonstrated that the distributions of Cpt are similar in the condition of high squealer. However, when the squealer height is small, with the increase of it, the spanwise range of high Cpt in LV is reduced, and that in UPV is enlarged obviously.

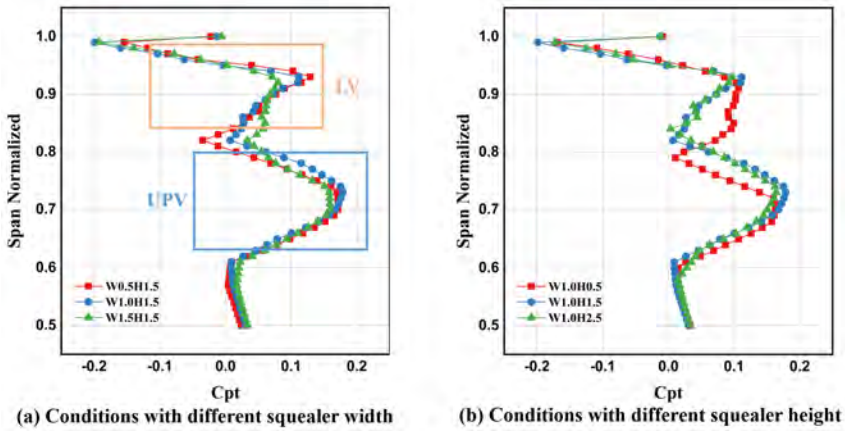

Figure 17 Distributions of pitch-wise mass-averaged total-pressure loss coefficient at the plane 30%Cax downstream of the rotor.

Fig.18 comparisons tip-leakage loss and turbine stage efficiency of different cavity tips, normalized by the case of W1.0H1.5. As shown in Fig.18, with the squealer width or height increase, tip-leakage loss fist increases and then decreases, and in consequent, the turbine stage efficiency first increases and then decreases. That is, there are optimum values of squealer width and height to perform best in aerodynamic performance. Based on the preceding discussions, it can be demonstrated that, in the conditions with narrow squealer, the enhancement of the SV influencing intensity is dominant in controlling tip-leakage loss; while in the conditions with wide squealer, the reduction of the SV influencing scope is dominant. The variation of leakage loss is similar to that with different squealer height conditions. Besides, according to Fig.18, it is illustrated that turbine aerodynamic performance is more sensitive to the variation of squealer width when large, while it takes place when the squealer height is small. As a whole, the influence of squealer height on turbine aerodynamic is more significant compared to squealer width.

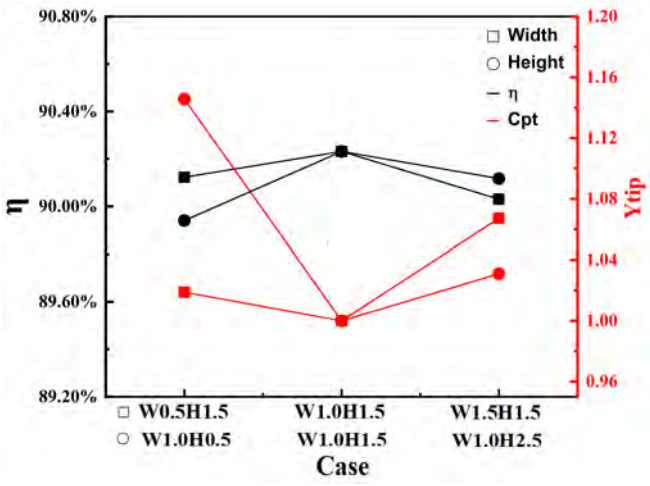

Figure 18 Comparison of aerodynamic performance of different cavity tips.

CONCLUSIONS

In this study, the influences of squealer width and height on the pressure distribution in the tip region, the evolution of dominant flow structure SV and turbine aerodynamic performance are investigated numerically, in a typical transonic high-pressure turbine stage with cavity tip. Several conclusions were drawn as follows:

- The variation of squealer width or height does not alter the evolution law of the SV, but changes the SV characteristics significantly. Along the cavity, the SV intensity decreases first and then increases, and the SV size increases first and then decreases accordingly. Meanwhile, the SV moves to the SSS gradually until flowing out of the cavity. The position of SV in the cavity is demonstrated as the critical characteristic on the control of the leakage flow. That is, the closer SV locates to the SSS and the later SV flows out of cavity in the meantime, the better the controlling effect on tip-leakage flow is generated.
- With the increase of squealer width, the TPG in the gap increases, and then the migration speed of the SV to the SSS slows down; but, due to the decrease of the width of the cavity, the position of the SV flowing out of the cavity is advanced. Meanwhile, the SPG decreases, and then the SV intensity is greater and the size smaller correspondingly. However, the enhancement of adverse TPG makes the amplitude of intensity increasing smaller, and that of size decreasing bigger. The influencing scope and size of SV are more sensitive to the variation of squealer width.
- With the increase of the squealer height, together with the decrease of the TPG in the gap, the SV is closer to the SSS, and flows out of the cavity earlier. In the meantime, the SPG in the cavity increases, and then the variation speed of the SV intensity and size along the streamwise direction slows down accordingly. Meanwhile, the enhancement of local adverse TPG produces a decreasing trend of vorticity and size. As a whole, the variation of squealer height has remarkable effect on all characteristics of SV.
- As the squealer width or height increases, the influencing scope of SV reduces, while the influencing intensity increases. Consequently, there are optimum values of squealer width and height leading to the best controlling effect on the tip-leakage loss. Turbine aerodynamic performance is more sensitive to the variation of squealer width when large, while it takes place when the squealer height is small. Compared to squealer width, the influence of squealer height on turbine aerodynamic is more significant.

NOMENCLATURE

Nomenclature

Latin letters

$\dot{m}$	Mass flow $[kg/s]$
A	Area $[m^2]$
h	Blade height $[m]$
l	Streamwise length $[m]$
n	Rotational speed $[rpm]$
P	Pressure $[Pa]$
T	Temperature $[K]$
V	Velocity $[m/s]$
Y	Leakage loss $[J]$

Greek letters

η	Isentropic efficiency [-]
ω	Vorticity $[s^{-1}]$
π	Expansion ratio [-]
ρ	Density $[kg/m^3]$
τ	Gap height $[m]$

Subscripts

1	Rotor inlet
2	Rotor outlet
$diff$	Difference
e	Equivalent
is	Isentropic
N	Normal direction
$notip$	Condition with no tip
tip	Condition with tip

ACKNOWLEDGMENTS

This investigation was supported by The National Natural Science Foundation of China (No. 51676005), which is gratefully acknowledged.

References

Bunker, R. S. (2006), 'Axial Turbine Blade Tips: Function, Design, and Durability', *Journal of Propulsion and Power* **22**(2), 271–285. Publisher: American Institute of Aeronautics and Astronautics.

Chen, G., Dawes, W. and Hodson, H. (1993), A numerical and experimental investigation of turbine tip gap flow.

Coull, J. D., Atkins, N. R. and Hodson, H. P. (2014), High Efficiency Cavity Winglets for High Pressure Turbines, American Society of Mechanical Engineers Digital Collection.

Denton, J. D. (1993), 'Loss Mechanisms in Turbomachines', *Journal of Turbomachinery* **115**(4), 621–656.

Du, K., Li, Z., Li, J. and Sunden, B. (2019), 'Influences of a multi-cavity tip on the blade tip and the over tip casing aerothermal performance in a high pressure turbine cascade', *Applied Thermal Engineering* **147**, 347–360.

Erhard, J. (2000), Design, Construction and Commissioning of a Transonic Test-Turbine Facility, PhD thesis.

Go¨ttlich, E., Neumayer, F., Woisetschla¨ger, J., Sanz, W. and Heitmeir, F. (2004), 'Investigation of Stator-Rotor Interaction in a Transonic Turbine Stage Using Laser Doppler Velocimetry and Pneumatic Probes', *Journal of Turbomachinery* **126**(2), 297–305.

Heyes, F. J. G., Hodson, H. P. and Dailey, G. M. (1992), 'The Effect of Blade Tip Geometry on the Tip Leakage Flow in Axial Turbine Cascades', *Journal of Turbomachinery* **114**(3), 643–651.

Lei, Q., Zhengping, Z., Huoxing, L. and Wei, L. (2010), 'Upstream wake–secondary flow interactions in the endwall region of high-loaded turbines', *Computers & Fluids* **39**(9), 1575–1584.

Maral, H., Şenel, C. B., Deveci, K., Alpman, E., Kavurmacıoğlu, L. and Camci, C. (2019), 'A Genetic Algorithm Based Multi-Objective Optimization of Squealer Tip Geometry in Axial Flow Turbines: A Constant Tip Gap Approach', *Journal of Fluids Engineering* **142**(2).

Mischo, B., Burdet, A. and Abhari, R. S. (2010), 'Influence of Stator-Rotor Interaction on the Aerothermal Performance of Recess Blade Tips', *Journal of Turbomachinery* **133**(011023).

Pátý, M., Cernat, B., De Maesschalck, C. and Lavagnoli, S. (2018), Experimental and Numerical Investigation of Optimized Blade Tip Shapes: Part II — Tip Flow Analysis and Loss Mechanisms, American Society of Mechanical Engineers Digital Collection.

Schabowski, Z., Hodson, H., Giacche, D., Power, B. and Stokes, M. R. (2014), 'Aeromechanical Optimization of a Winglet-Squealer Tip for an Axial Turbine', *Journal of Turbomachinery* **136**(071004).

Senel, C. B., Maral, H., Kavurmacioglu, L. A. and Camci, C. (2018), 'An aerothermal study of the influence of squealer width and height near a HP turbine blade', *International Journal of Heat and Mass Transfer* **120**, 18–32.

Virdi, A. S., Zhang, Q., He, L., Li, H. D. and Hunsley, R. (2015), 'Aerothermal Performance of Shroudless Turbine Blade Tips with Relative Casing Movement Effects', *Journal of Propulsion and Power* **31**(2), 527–536. Publisher: American Institute of Aeronautics and Astronautics.

Young, J. B. and Wilcock, R. C. (2002), 'Modeling the Air-Cooled Gas Turbine: Part 2—Coolant Flows and Losses', *Journal of Turbomachinery* **124**(2), 214–221.

Zeng, F., Du, J., Huang, L., Xuan, L., Zhao, Q. and Zou, Z. (2020), 'An experimental method for squealer tip flow field considering relative casing motion', *Chinese Journal of Aeronautics* **33**(7), 1942–1952.

Zhou, C. (2015), 'Effects of endwall motion on thermal performance of cavity tips with different squealer width and height', *International Journal of Heat and Mass Transfer* **91**, 1248–1258.

Zhou, C. and Hodson, H. (2012), 'Squealer Geometry Effects on Aerothermal Performance of Tip-Leakage Flow of Cavity Tips', *Journal of Propulsion and Power* **28**(3), 556–567. Publisher: American Institute of Aeronautics and Astronautics.

Zou, Z., Shao, F., Li, Y., Zhang, W. and Berglund, A. (2017), 'Dominant flow structure in the squealer tip gap and its impact on turbine aerodynamic performance', *Energy* **138**, 167–184.

Zou, Z., Wang, S., LIU, H. and Zhang, W. (2018), *Axial Turbine Aerodynamics for Aero-engines: Flow Analysis and Aerodynamics Design*, Springer Singapore.

Zou, Z., Xuan, L., Chen, Y. and Shao, F. (2020), 'Effects of flow structure on heat transfer of squealer tip in a turbine rotor blade', *International Communications in Heat and Mass Transfer* **114**, 104588.